



Larval description and developmental staging of *Amolops* tadpoles from Nepal, including ultrastructure of the oral disc and sucker

MOHSEN NOKHBATOLFOGHAHAI¹, KEVIN W. CONWAY², LIAM ATHERTON¹, PREM B. BUDHA³,
MICHAEL J. JOWERS⁴ & J. ROGER DOWNIE¹

¹) School of Life Sciences, Graham Kerr Building, University of Glasgow, Glasgow, UK

²) Department of Ecology and Conservation Biology, Biodiversity Research and Teaching Collections, Texas A & M University, College Station, Texas 77843, USA

³) Central Department of Zoology, Tribhuvan University, Kirtipur, Kathmandu, Nepal

⁴) CIBIO/InBIO, Research Centre in Biodiversity and Genetic Resources, Porto University, Campo de Vairão, Vairão, Portugal

Corresponding author: MICHAEL J. JOWERS, e-mail: michaeljowers@hotmail.com

Manuscript received: 23 December 2019

Accepted: 21 July 2020 by JÖRN KÖHLER

Abstract. Tadpoles of the Asiatic torrent frog genus *Amolops* possess large abdominal suckers and a complex oral apparatus which allow them to adhere tightly to and also to move over wet rock surfaces, a morphology termed gastromyzophorous. Accounts of larval development, and overall sucker morphology and microstructure are patchy in this genus. Here, from a large sample (n = 90) of *Amolops* tadpoles collected from two sites in Nepal, we give a detailed description of the tadpoles' external morphology, including pigment pattern variation, and their development from soon after hatching to the approach of metamorphosis, including new features of their oral apparatus (tooth rows and labia). Using SEM, we describe ultrastructural details of the sucker's surface, especially microvillated cells of the friction areas. From stained sections, previously unreported arrays of elastin fibres are described from the distal margins of the suckers. Based on our phylogenetic analyses and tadpole morphology we conclude that our specimens belong to the recently described species, *A. mahabharatensis*.

Key words. Amphibia, Anura, Ranidae, adhesion, histology, SEM, phylogeny, Himalayas.

Introduction

The ranid genus *Amolops* currently contains over 50 species (FROST 2020) distributed across the mountainous regions of south east Asia, including northern India, Nepal, western and southern China, Malaysia and Vietnam. The taxonomic and conservation status of several of these species are data deficient (FROST 2020, AmphibiaWeb 2019). All live along fast-flowing streams, and are characterised by having gastromyzophorous tadpoles which possess a substantial abdominal sucker, a highly muscular tail and reduced tail fins. The gastromyzophorous morphotype is one of the 18 ecomorphological guilds of exotrophic anurans distinguished by ALTIG & JOHNSTON (1989), occurs in several genera of the families Bufonidae and Ranidae, and has therefore presumably evolved at least twice independently (GAN et al. 2015). The phylogenetic relationships of the three genera of ranid cascade frogs with gastromyzophorous tadpoles (*Amolops*, *Huia* and *Meristogenys*) remain unresolved (GAN et al. 2015).

NOBLE (1929) provided a detailed account of the anatomy of the sucker and its underlying musculature. Unfortunately, Noble referred his specimens to the genus *Stauroidis*, an error which caused confusion for decades (NGO et al. 2006): *Stauroidis* tadpoles are not gastromyzophorous.

There are few accounts of the development of *Amolops* embryos and larvae. HORA (1932) provided illustrations of some embryonic and larval stages of *Rana afghana* (= *Amolops afghanus*), with details on the cement gland's early role in adhesion. PHAM et al. (2015) described the developmental sequence of *A. cremnobatus* (from Vietnam), covering a selection of GOSNER (1960) stages from cleavage through to metamorphosis. Eggs were large, about 3 mm in diameter, each enclosed in a thick adhesive jelly layer and stuck to wet rocks as coherent clutches of 10–30 eggs, regularly washed over by stream water. Larvae released themselves from the jelly capsule at stage 24–25 and remained strongly attached to the rock surface by their suckers, with some adhesive jelly remaining while they increased in length from about 9.5 to 25.4 mm. PHAM et al. (2015) found

that tail shortening was apparent by stage 37 (these measurements, however, were based on single specimens). The oral apparatus and sucker remained intact throughout the larval stages, but at stage 42, the lower tooth rows began to regress.

In this paper, we report on larval development (stages 25–36) in a large sample of *Amolops* collected in central Nepal. According to SCHLEICH & KÄSTLE (2002), four *Amolops* species occur in Nepal: *A. marmoratus*, *A. monticola*, *A. nepalicus*, *A. formosus*. They provide diagnostic features, particularly oral disc characteristics, for three of the tadpole species, but not for *A. formosus*. Recently, KHATIWADA et al. (2020) have described a new species, *A. mahabharatensis* from Nepal, and also briefly describe its tadpole. We have examined the *Amolops* tadpole collections from Nepal in the Natural History Museum, London (NHM), and in the Discussion consider the identity of the tadpoles described in this paper. We report new details on the oral apparatus and abdominal sucker, based on both light and scanning electron microscopy, as well as a description of the larvae. Finally, we present a molecular phylogenetic analysis based on DNA extracted from an ethanol-preserved specimen, as an aid to identifying the species our specimens belong to, and to place it in its evolutionary context.

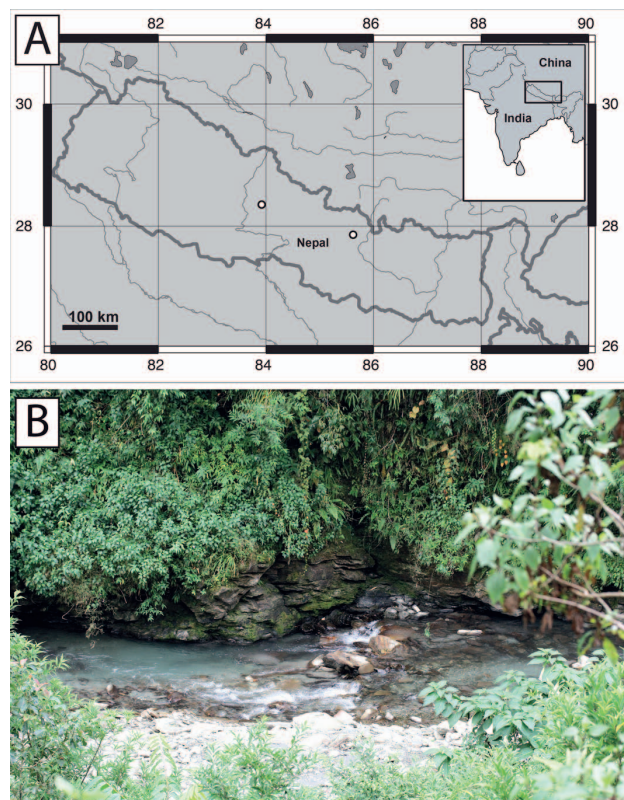


Figure 1. A) Sampling localities for *Amolops* specimens used in this study. B) Phathi River, one of the fast-flowing streams where *Amolops* specimens were captured.

Materials and methods

Specimen collection and preservation

Tadpoles ($n = 90$) were collected from two locations in Nepal during October and November 2008: the Indrawati River at Melamchi Township, Bagmati Zone, downstream of the confluence with Melamchi River ($+27^{\circ}49'42.50''$ N, $+85^{\circ}34'37.10''$ E), and the Phathi River, downstream from the Phathi Khola bridge on the road from Pokhara to Baglung, Gandaki Zone ($+28^{\circ}17'9.90''$ N, $+83^{\circ}51'45.90''$ E). The tadpoles were collected as bycatch during general diversity surveys of hillstream fishes in central Nepal (e.g., CONWAY et al. 2011). Typical habitat is shown in Figure 1. Tadpoles were caught in a 2×2 m seine net, mesh size about 3×3 mm, stretched across each stream. One of our collecting team walked down the stream towards the net, kicking the gravelly and stony substrate; both fish and tadpoles swam into the net as a result of this disturbance. Immediately after capture, a few tadpoles were transferred to a glass photoaquarium containing clean water so that their colours in life could be recorded. Captured tadpoles were anaesthetised in a dilute solution of clove oil in water (about 5mg per litre: MITCHELL 2009, JAVAHERY et al. 2012), then preserved in 10% formalin, with a few in ethanol for DNA analysis (Phathi River sample only).

Specimens have been deposited in the following collections: University of Glasgow's Hunterian Zoology Museum (GLAHM 161993, 23 specimens, Indrawati River; GLAHM 161994, 16, Phathi river); the Biodiversity Research and Teaching Collections at Texas A & M University, College Station (TCWC 104887, 5, Indrawati River; TCWC 104888, 5, Phathi River); and the Central Department Zoology Museum of Tribhuvan University, Kathmandu (CDZM-TU A2077-1, 15, Indrawati River; A2077-2, 15, Phathi River).

Developmental staging and gross morphology

Morphological features were examined on 50 Indrawati and 36 Phathi River fully intact specimens with the aid of a dissecting microscope and measured using dial callipers accurate to 0.1mm. Each tadpole was staged using GOSNER (1960). We used the labial tooth row formula (LTRF), morphological terminology and measurements recommended by ALTIG & McDIARMID (1999). To check for any individual and developmental differences in pigmentation patterns, we examined all specimens from both locations separately at stages 28, 31 and 35 (stages at which we had five or more specimens from each location). In addition to examining our collection from Nepal, we examined preserved tadpoles from Nepal and northern India in the NHM.

Scanning electron microscopy (SEM)

We used SEM to examine the fine structure of the surface of the abdominal sucker and of the oral disc. Suckers and

discs were cut from formalin-preserved tadpoles at stages 27, 28 and 31, treated with 2.5% glutaraldehyde in phosphate buffer for 5 hours, rinsed in phosphate buffer, then post-fixed in 1% osmium tetroxide in 0.5% aqueous uranyl acetate for 1 hr. Specimens were then dehydrated through an acetone series and critical point dried with liquid CO₂ in a Polaron critical point drier. They were mounted on aluminium stubs using double-sided copper tape and coated with gold/palladium to a thickness of approximately 20 nm using a Polaron SC515 coating system. Specimens were examined using a JEOL 6400 SEM at 6Kv over a magnification range of 20–10,000 times, and images were captured using Scandium SEM imaging software.

Paraffin wax sections

To examine the internal structure of the oral apparatus and sucker, whole tadpole bodies (stage 28) or dissected pieces of tissue were processed for paraffin wax histology using standard methods. Sections were cut at 5–7 micrometres and stained using Haematoxylin, Eosin and Alcian Blue, Mallory's Trichrome or Van Gieson's method for elastic fibres as modified by MILLER (1971). Sections were examined using a Leitz microscope and images recorded using Adobe Photoshop V.7 software.

DNA analysis

We sequenced DNA from one *Amolops* sp. tadpole tail tip for possible genetic identification. Whole genomic DNA was extracted using the DNeasy Blood & Tissue kit (QIAGEN, Hilden, Germany) following the manufacturers' instructions or with the standard high-salt protocol of SAMBROOK et al. (1989). We used one mitochondrial gene fragment, 12S rDNA with primers L1091 (KOCHER et al. 1989) and AMOL-12R GAAGAGGGTGACGGGCGGT (this study). We downloaded all *Amolops* 12S rDNA sequences from Genbank (n = 137) but the final alignment only included representative lineages per clade and at least one individual per species (n = 41). In order to sample all possible diversity within *Amolops*, when more than one species showed high divergence, and occasional paraphyly, it was also included in the alignment. We used *Nanorana quadranus* and *Fejervarya limnocharis* as the outgroup (CAI et al. 2007).

Seaview v.4.2.11 (GOUY 2010) was used for preliminary alignments of sequences and were aligned thereafter in MAFFT (KATOH et al. 2002), and phylogenetic analyses were conducted using 440 base pair (bp) alignment (the *Amolops* sequence was 337 bp long). The most appropriate substitution model (TIM2+I+G) was determined by the Bayesian Information Criterion (BIC) in jModeltest 2 (POSADA 2008). Phylogenetic relationships between taxa were inferred using the Bayesian Inference (BI) optimality criterion under the best fitting substitution model. MrBayes v3 (RONQUIST & HUELSENBECK 2003) was used with

default priors and Markov chain settings, and with random starting trees. Each run consisted of four chains of 20 million generations, sampled every 10,000 generations. Phylogenetic relationships were also estimated using a Maximum Likelihood (ML) approach, as implemented in the software RAxML v7.0.4 (SILVESTRO & MICHALAK 2012), under the best partition scheme under the GTR model. All analyses were performed using the CIPRES platform (MILLER et al. 2010).

Results

External and internal morphology and morphometrics

Although individual variation in pigmentation was apparent, in all other respects, our sample was uniform enough to assume that they all belonged to the same species. The descriptions and measurements presented here are based on three stage 35 tadpoles and a stage 26/27 tadpole for oral apparatus morphology (Figs 2, 3; Table 1). Quantitative differences across the sample are given in the section on larval staging.

Pigmentation and behaviour in life: Tadpoles in the photoaquarium readily attached to the aquarium side below the water surface, allowing photographs to be taken of dorsal and ventral surfaces. They did not move around. In life, the dorsal side was brown/black mottled with small orange/yellow patches; the ventral side of the body white/grey (Figs 2A, B).

In the preserved state, using a stage 35 tadpole as an example, the lateral surface of the body is grey with irregular small dark spots; the body of the tail is grey with irregular and individually variable large white blotches; tail fins



Figure 2. Living specimen of an *Amolops* tadpole from Phathi River attached to the side of an aquarium in dorsal (A) and ventral (B) views: limb buds indicate stage 34. Image reversed in A). Specimen likely now contained in GLAHM 161994.

Table 1. Morphometrics of *Amolops* sp. tadpoles: means of measurements (mm) from three Indrawati individuals at GOSNER (1960) stage 35 (GLAHM 161993). Features as defined by McDIARMID & ALTIG (1999), except sucker dimensions.

Feature	Mean measurement	% of total length
Total length	41.6	–
Body length	14.6	35.1
Tail length	27.0	64.9
Tail muscle height	4.6	11.1
Tail muscle width	4.8	11.5
Maximum tail height	6.6	15.9
Interorbital distance	5.2	12.5
Internarial distance	2.8	6.7
Upper jaw sheath length	3.2	7.7
Upper jaw sheath width	0.4	1.0
Sucker: internal length	5.9	14.2
Sucker: internal width	6.4	15.4

are mottled grey with white patches at the outer edges. The dorsal surface of the body is grey, with irregular small dark spots, as on the lateral surfaces (Figs 3A, B). The ventral surface of the body is mainly cream/white (Fig. 3C). Individual and developmental differences in pigmentation patterns are described later.

Tail: At the tail/body junction, the tail is highly muscular and bears negligible dorsal and ventral fins. The dorsal fin becomes apparent a short distance along the tail and widens to a maximum about midway along the tail; the ventral fin starts further posteriorly, widening to a maximum nearer the tail tip, but is never as wide as the dorsal fin. The tail narrows to a sharp tip, with the muscular and skeletal elements extending almost to the tip (Fig. 3A).

Body: The body occupies a little over one third of the tadpole's total length, and is dorso-ventrally flattened. The eyes are large, dorsal and directed laterally; nares are dorsal, oval, with the longer axis anterior–posterior (Fig. 3D): they have a small mid-dorsal protuberance and lie slightly nearer the eyes than the tip of the snout; the spiracle is single, low on the left side, just posterior to the rear end of the sucker (Figs 3B, C); the vent tube is central, mid-way

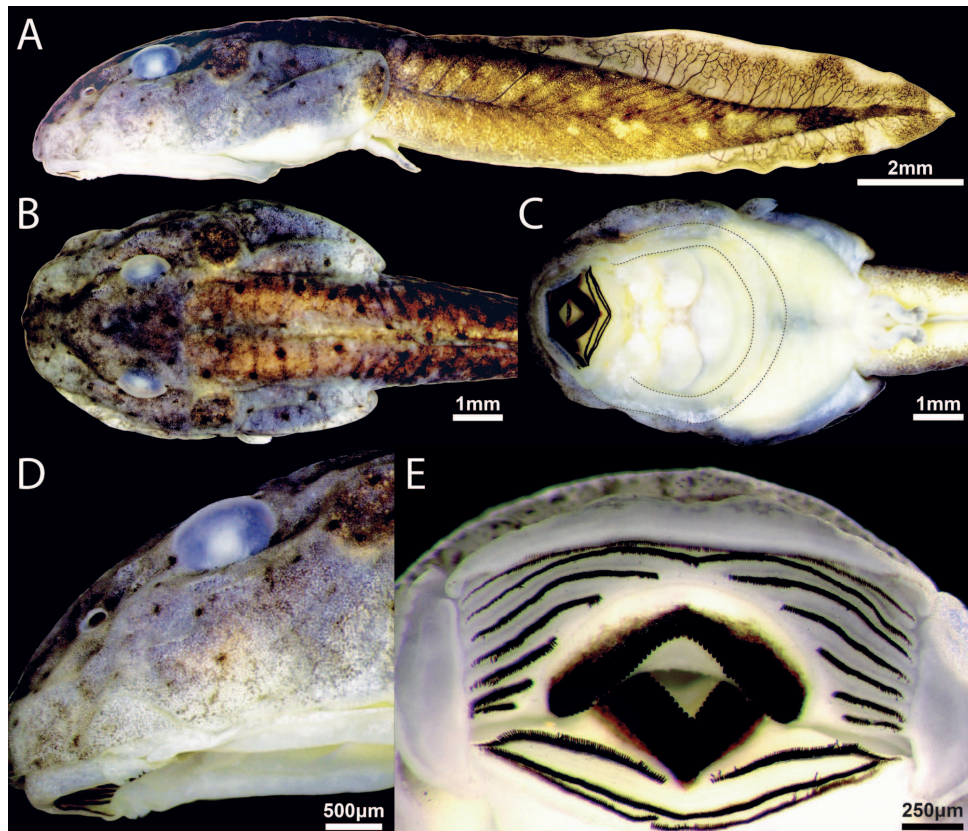


Figure 3. Preserved specimen of an *Amolops* tadpole, stage 35, from the Indrawati River (GLAHM 161993). A) lateral view (right side, image reversed) showing asymmetry and posterior origin of tail fins, eye and nostril positions; B) dorsal view of body with spiracle protruding from the left side; C) ventral view of the body (margin of abdominal sucker outlined with dashed line) and anterior tail: spiracle protruding at level of sucker posterior rim; D) detail of head showing eye and nostril; E) oral apparatus (anterior to top of page) showing prominent jaws, labia and tooth rows: anterior labium with fringe of small teeth, followed by seven main tooth rows; lateral labia with papillae; posterior labium with three tooth rows; narrow gap separates lateral labia from both anterior and posterior.

between the limb buds. The ventral surface of the body is occupied, from the anterior end, first by the oral apparatus (about one quarter of the body in length), immediately followed by the sucker (about half the body's length), and then abdominal skin, ending at the junction of body and tail where the limb buds protrude.

Oral apparatus (Fig. 3E): The oral apparatus is ventral and large, but not as wide as the body; the labial tooth row formula (LTRF) is 8(4–8)/3(1). However, an unusual feature is the first anterior (A1) row, which is situated at the edge of the anterior labium, and has teeth noticeably short-

er and finer than those elsewhere on the oral disc (Figs 4A–C). Row A1 extends the full length of the anterior labium. The remaining anterior tooth rows are situated on raised, laterally orientated ridges, terminating laterally at the bases of the lateral labia and medially close to the beak. The first posterior tooth row is sub-divided, terminating medially close to the beak; the other two posterior rows are continuous. The wide flat lateral labia each bear a single row of short finger-like papillae at their outer edges. Papillae are otherwise absent from the oral apparatus. There is a narrow gap between the lateral and both anterior and poste-

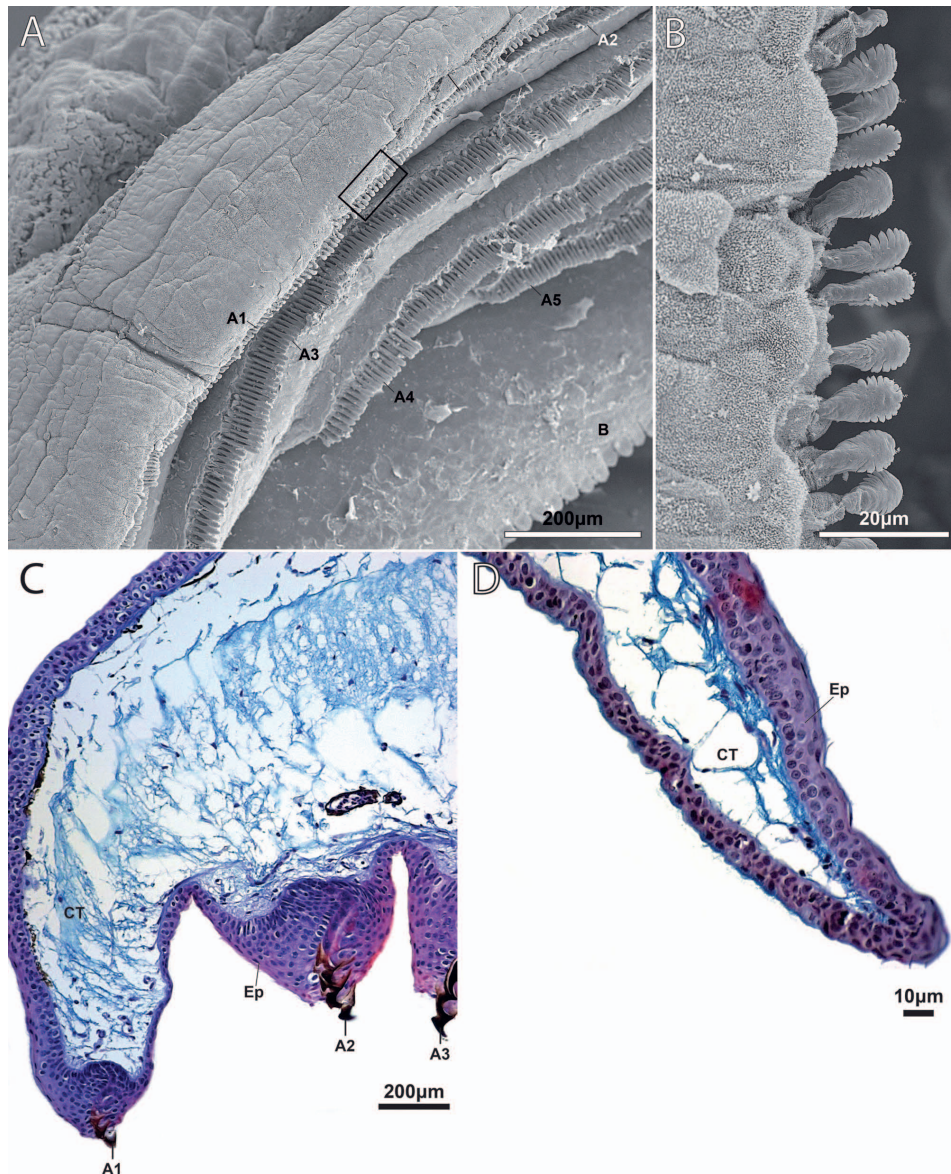


Figure 4. Low (A) and high (B) resolution SEMs of the anterior labium and keratodont tooth rows A1–5 (specimen from GLAHM 161993). A) Anterior labium with the small teeth of keratodont row A1 protruding to the right; below on the right are rows A2–5, showing much longer teeth; to the far right is the serrated edge of the beak. Box shows approximate area of A1 row shown at higher magnification in B). C) Haemalum, eosin and alcian blue-stained section of anterior labium showing labium edge with A1 keratodont row, then rows A2 and A3 with more substantial teeth and generative tissue. D) Haemalum, eosin and alcian blue-stained section of posterior labium edge, lacking teeth. Abbreviations: A1–5, keratodont tooth rows 1–5; B, beak; CT, connective tissue; Ep, epidermis.

rior labia, best seen in Figures 3E and 5A–C. The posterior labium is a wide flat flap, projecting over the anterior surface of the sucker. It has no teeth (Fig. 4D). The jaw sheaths of the beak are highly keratinised and black with uniformly serrated edges; the upper jaw sheath is single, not divided.

Abdominal sucker: The sucker is nearly as wide as the body and extends to three-quarters the length of the body.

Figure 5 shows low and intermediate resolution SEM views of the abdominal sucker at stages 27, 28 and 31. There are no obvious differences between the three stages, except in size. The main expanse of the sucker (the floor) is surrounded laterally and posteriorly by a raised rim. The floor is divided into anterior and posterior regions by a M-shaped indentation or fold. Anteriorly, the rim widens as it meets the

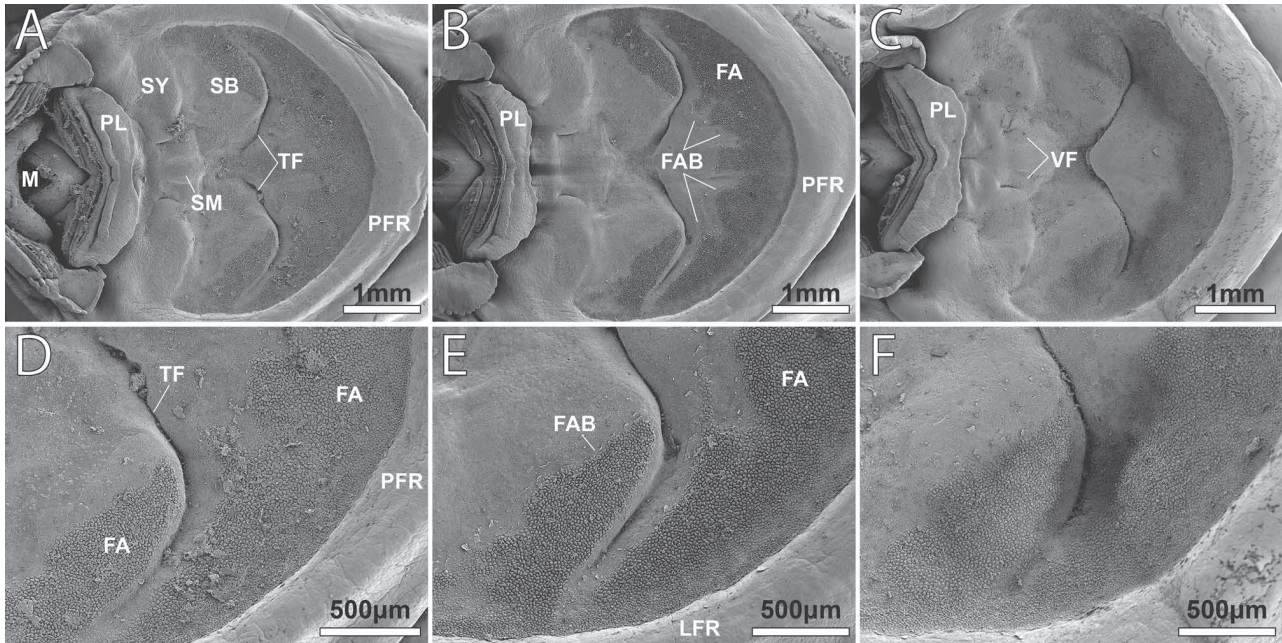


Figure 5. Low (A–C) and intermediate (D–F) resolution SEMs of *Amolops* tadpole ventral body surfaces showing oral apparatus and sucker (specimen from GLAHM 161993). A, D) stage 27; B, E) stage 28; C, F) stage 31. D–F) focus on the friction area of the sucker. S labels show positions of underlying muscles (SB, sub-branchial; SM, sub-maxillary; SY, sub-hyoideus). Abbreviations: FA, friction area; FAB, friction area border; M, mouth; LFR, lateral free rim; PFR, posterior free rim; PL, posterior labium; TF, transverse folds; VF, vertical folds.

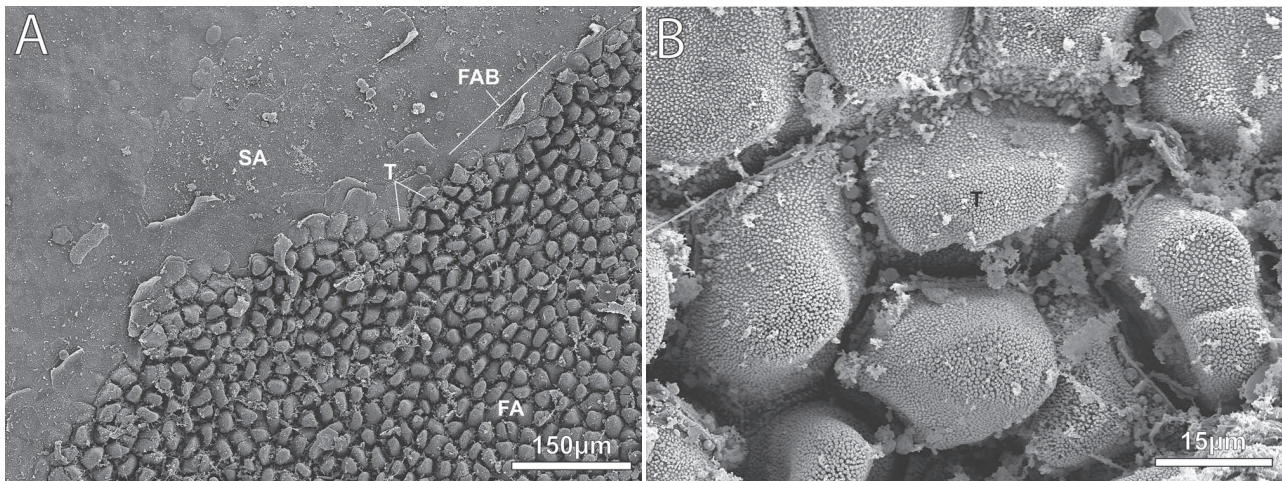


Figure 6. A) High resolution SEMs of the friction area surface of an *Amolops* tadpole sucker (specimen from GLAHM 161993). B) Tubercles at higher magnification, showing their microvillar structure. Abbreviations: FA, friction area; FAB, border of friction area; SA, smooth area; T, tubercles.

posterior labium of the oral apparatus. On the floor, close to the posterior labium are a pair of short anterior–posterior indentations. The lateral and posterior surfaces of the sucker floor are covered by a wide band of small rounded cells (Fig. 6A). At higher resolution (Fig. 6B), these rounded cells are seen to be covered in microvilli. Elsewhere, the surface of the floor is smooth, even at high resolution.

Figure 7A shows a low-resolution transverse section through the head (stage 28, posterior eye level) of a tadpole, including the abdominal sucker. The sucker rims are hollow protrusions from the sides of the sucker. When examined at higher resolution (Fig. 7C), the rim is covered by a stratified epithelium, underlain by a prominent basal lamella. The interior of the rim appears devoid of cells, but contains

some amorphous material. The surface of the sucker floor is a stratified epithelium, underlain by a basal lamella, and then a mass of dense connective tissue (Fig. 7B). The thickness of the epithelium varies with location: thick in the regions with surface rounded cells, thin at folds on the sucker floor. Using Van Gieson staining to highlight elastin fibres, we see that the connective tissue at the junction between the sucker floor and the rim is highly enriched with thin, black elastin fibres (Fig. 7D). The remainder of the connective tissue contains sparse cells and many long connective tissue fibres, most likely collagen, that are orientated mainly in a dorsal–ventral direction. The surface of the sucker floor is either smooth, or rough with tubercles peripherally, where the rounded cells seen in SEM occur.

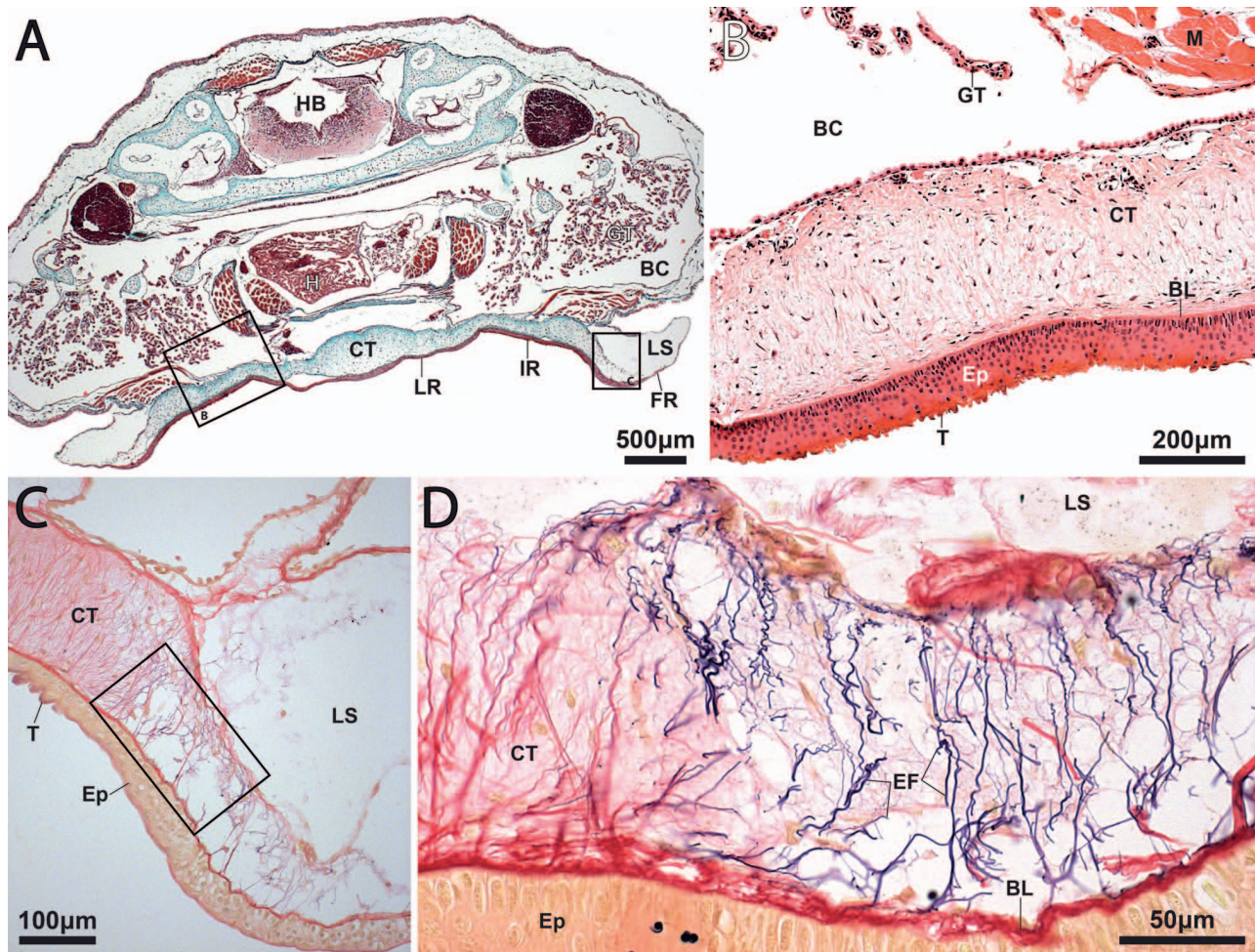


Figure 7. Stained cross sections of a stage 28 *Amolops* tadpole (specimen from GLAHM 161993). A) Mallory-stained section through posterior edge of eyes, heart, gills and sucker. Boxes indicate approximate areas shown at higher magnification in B) and C). B) Intermediate resolution haemalum and eosin-stained view of the friction area of the sucker (intermediate region) showing stratified epidermis, thick connective tissue layer, branchial chamber and adjacent muscle. C) Van Gieson-stained higher resolution view of the junction between the friction area of the sucker (left), underlain by a thick connective tissue layer, and the free rim (right). Box shows approximate area shown at higher magnification in D). D) Van Gieson-stained high resolution view of the sucker (left) / free rim (right) junction, showing abundance of black-stained elastin (EF) fibres at the junction, and connective tissue with no elastin deep to the sucker. Abbreviations: BC, branchial chamber; BL, basal lamella; CT, connective tissue; EF, elastic fibres; EP, epidermis; FR, free rim of sucker; GT, gill tissue; H, heart; HB, hindbrain; IR, intermediate region of sucker; LR, lobe region of sucker; LS, sinus in middle of sucker rim; M, muscle; T, tubercle.

Table 2. Dimensions of *Amolops* sp. tadpoles arranged by GOSNER (1960) stage (measurements as mm, given as mean \pm SD); Phathi and Indrawati samples combined. See Supplementary document S1 for the two samples shown separately.

Stage	n	Total length	Body length	Body/total length (%)	Sucker width	Sucker width/total length(%)
25	1	15.4	7.1	46.1	4.0	26.0
26/7	2	22.8 \pm 1.9	9.1 \pm 1.0	39.9	5.5 \pm 0.5	24.1
27/8	6	24.0 \pm 2.1	9.1 \pm 0.8	37.9	4.8 \pm 0.7	20.0
28	13	27.1 \pm 2.5	9.8 \pm 0.5	36.2	5.4 \pm 0.6	19.9
28/9	2	29.3 \pm 1.1	10.6 \pm 0.4	36.2	6.0 \pm 0.1	20.5
29	8	29.7 \pm 1.7	11.0 \pm 0.4	37.0	6.2 \pm 0.5	20.9
29/30	3	29.6 \pm 0.9	11.0 \pm 0.5	37.2	6.3 \pm 0.7	21.3
30	2	35.2 \pm 3.0	12.5 \pm 0.5	35.5	7.1 \pm 1.0	20.2
30/1	6	34.3 \pm 2.8	11.7 \pm 0.9	34.1	6.1 \pm 0.3	17.8
31	7	34.4 \pm 1.7	12.3 \pm 0.7	35.8	6.8 \pm 0.6	19.8
32	5	38.0 \pm 1.8	12.8 \pm 0.6	33.7	7.2 \pm 0.9	18.9
32/3	1	40.9	13.7	33.5	8.2	20.0
33	1	41.4	14.6	35.3	8.0	19.3
34	6	41.1 \pm 2.7	13.9 \pm 1.6	33.8	7.7 \pm 0.9	18.7
34/5	1	41.8	13.6	32.5	7.0	16.7
35	15	42.1 \pm 1.7	14.6 \pm 0.9	34.7	8.0 \pm 0.7	19.0
35/6	2	42.4 \pm 1.6	15.0 \pm 0.8	35.4	8.6 \pm 0.7	20.3
36	5	45.6 \pm 2.3	15.6 \pm 0.6	34.2	8.9 \pm 0.6	19.5

NHM specimens: The specimens we examined were all labelled as *Amolops afghanus*, and had been collected from Nepal (1962), Sikkim (1915), Darjeeling (1889), the Khasi Hills (1929) and Dharmasala (1926). The LTRF in all cases was 8(4–8)/3(1), identical to our Nepal sample.

Larval staging

Our sample ranged from GOSNER (1960) stages 25 to 36. The staging system depends heavily on hind limb development, and we sometimes found specimens which fell between two stages. Table 2 catalogues the stages found, and their dimensions: total length, body length, and sucker width. The Table combines the data from all the specimens measured. In Supplementary document S1, we show the data from the two locations separately. Size at any one stage was variable; for example, at stage 28, the 12 specimens ranged from 23.1 to 30.4 mm in total length; and at stage 35, 15 specimens ranged from 38.1 to 44.2 mm. Body proportions changed most over the earlier stages, with the ratio body length/total length 46.1% at stage 25, but 37% or less at later stages. Similarly the relative size of the sucker (sucker width over total body length) reduced from 26% at stage 25 to less than 20% at later stages.

Individual and developmental differences in preserved pigmentation patterns

We summarised the pigmentation pattern of a stage 35 tadpole earlier. Here we provide detail on variations. At each

stage examined (28, 31 and 35), we found a predominant pattern, the same at both sample locations, but with some individual variation. There appeared to be some overall differences between stage 28 and the later stages, but because we cannot tell whether our samples derived from the same or different batches of eggs, we cannot be sure whether these differences are developmental or not. There were no consistent differences between the specimens from the two locations.

In all cases, the ventral surfaces of the body and tail are melanocyte free and pale. Differences in melanocyte patterns are confined to the dorso-ventral surfaces. At stage 28, it is common for the tail fins to be transparent and pigment-free, except along the blood vessels. The body of the tail may be uniformly dark with close-packed melanocytes; but in a few specimens, there is an irregular pattern of pale blotches between the dark areas. The blotches are areas with very low densities of melanocytes and are about 1 mm in diameter, irregular in shape as well as arrangement, and the pattern differs between left and right sides. The main body surface is uniformly dark, again with close-packed melanocytes, but additionally shows a fairly regular pattern of small dark dots. These are composed of very densely packed melanocytes and are about 1 mm apart. In a few specimens, pale blotches, like those on the tail, also occur on the body; in these specimens, the small dark dots are generally absent.

At stages 31 and 35, most specimens show more patterning on the tail fins with pale blotches interspersed between the darker blood vessel networks, especially at the outer margins of the fins. The body of the tail has pale blotches in all cases. On the main body, the fairly regular pattern of

very dark spots against a dark background is predominant, although the sizes of the spots vary between individuals. The spots may also extend into the body of the tail. In some specimens, there are blotches instead of dark spots, but in a very few cases, spots and blotches co-occur.

DNA analysis

The 12S rDNA (337 bp) sequence (GenBank accession MT725736) matched with circa 88% to *A. marmoratus*, *A. panhai* and *A. indoburmanensis*, revealing that the studied species is not closely related to any of these. The phylogenetic analyses recovered a well-supported monophyletic clade with the new individual sequence within the *A. marmoratus* group (Fig. 8).

Discussion

Morphology and morphometrics: In general, the *Amolops* tadpoles we describe here are similar to those of other species of ranid gastromyzophorous tadpoles in having highly muscular tails with reduced fins (although the dorsal fin in our sample is more prominent than in some others), bodies compressed dorso-ventrally, large dorsal eyes, ventral oral apparatus with enlarged labia and multiple tooth rows, and, most characteristically, a large abdominal sucker (NOBLE 1929, YANG 1991, GAN et al. 2015). The sucker is surrounded posteriorly and laterally by a raised rim; the internal sucker surface has a peripheral posterior and lateral area of rough surface cells, characterised by NOBLE (1929)

as friction areas; elsewhere, the surface cells are smooth, but the surface has raised areas and deep folds. However, our results provide some details not previously reported, to our knowledge: these may be particular to the species we have studied, but have arisen from the methods we have used. In particular, our study appears to be the first to have used SEM for the examination of *Amolops* tadpoles. The features we wish to highlight are:

The first anterior tooth row (A_1) is borne on the outer margin of the anterior labium (Fig. 3 E), not on a ridge arising from the surface of the oral disc. The teeth of this row remain small throughout the larval stages, unlike the teeth on other rows.

The labia are divided into anterior, lateral and posterior, with only the lateral labia bearing a single row of papillae. There are narrow channels separating the lateral labia from both anterior and posterior labia. HORA (1930) felt that these channels might aid respiration, but his later investigation (HORA 1934) showed that respiratory currents entered via the nostrils and exited via the spiracle.

The rounded surface epidermal cells of the sucker friction areas are microvillated, presumably enhancing their friction role.

SEM renders the folds in the sucker surface especially prominent. NOBLE (1929) noted that the directions and locations of the surface folds differed between the species he examined (*A. ricketti* and *A. afghanus*, both *Stauroids* in his account). He suggested that these folds provide capacity for the sucker surface to stretch.

The finding of abundant elastin fibres at the sucker rim/surface junction is new. No-one appears to have previously used the Van Gieson method on these tissues. It is reason-

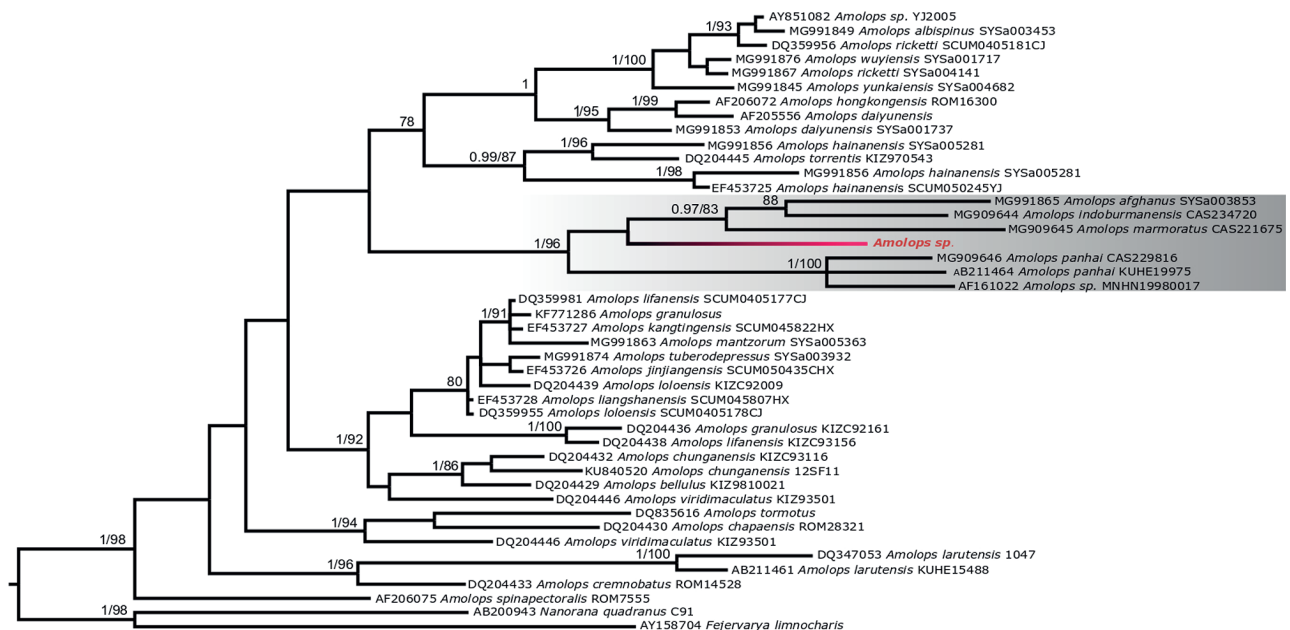


Figure 8. The best ML tree for all *Amolops* 12S rDNA sequence lineages (440 bp). Values by nodes indicate ML bootstrap support (> 75%) and Bayesian inference posterior probabilities (> 0.95), respectively. The red branch and taxon name show the sequenced *Amolops* specimen for this study. In grey is the *Amolops marmoratus* group.

able to deduce that elasticity at this point is helpful to sucker function, perhaps especially when a tadpole is moving along its substrate.

Adhesion and locomotion: The evolution and use of a sucker as an adhesive organ has been reported among the vertebrates from several groups of fishes and anuran larvae. GREEN & BARBER (1988) used SEM to investigate the suckers of clingfish (*Gobiesox maeandricus*), and their work has been supplemented by WAINWRIGHT et al. (2013) and DITSCHKE & SUMMERS (2019). The sucker is derived from modified pectoral and pelvic fins, plus the ventral epidermis: together, these create an outer seal when the sucker is closely applied to a substrate. Strength of adhesion decays with time, but is recovered by muscle action. Proximal to the outer rim is a zone of papillae, each with a hierarchical structure similar to the adhesive pads of geckos, i.e. subdivided into tiny setae or microvilli. Experiments have shown that the papillae are vital to the ability of clingfish to adhere to rough surfaces by adapting to the surface's irregularities, reducing leakage of the vacuum, and by increasing friction.

The surface structure of the clingfish sucker has similarities to those of gastromyzophorous tadpoles, especially the outer rim and the papillae. However, an important difference is that adhesion in these tadpoles is bi-modal, allowing movement across a substrate while remaining attached to it. HORA (1930, 1934) gave pioneering accounts of how the combined actions of the oral apparatus and sucker allowed both adhesion and progression. GAN et al. (2015) have extended these observations using modern methods. Essentially, opening of the jaws pushes the anterior labium forwards over the substrate; this movement also most likely relaxes the sucker's seal at the oral apparatus/sucker junction, allowing the body to be pulled forward. HORA (1930, 1934) emphasised the importance of the teeth, especially anterior row one at the tip of the anterior labium, in providing grip during the progression process. We wonder whether the channel between anterior and lateral labia also aids these movements. Whether or not suction is the sole adhesive mechanism for both sucker and oral apparatus has yet to be determined. *Amolops* tadpoles are capable of adhering both underwater and out of water on wet rocks, where they browse on surface biofilms in the splash zone (HORA 1934, MATSUI et al. 2006, PHAM et al. 2015). *Amolops* adults possess adhesive pads, similar to those of tree frogs, at the distal ends of their digits (YANG 1991), and their structure has been reported by OHLER (1995). Research on adhesion in some adult torrent frogs (not yet on *Amolops*) shows that they are well able to adhere to rough wet surfaces, but that they slip on smoother surfaces (ENDLEIN et al. 2013). The surface microstructure of these pads has some similarities to the frictional areas of gastromyzophorous tadpole suckers (DROTLEF et al. 2015), suggesting the hypothesis that the evolution of suckers has involved novel expression in the larvae of features found in ancestral adults, and that they are a characteristic derived from sucker-less forms such as *Staurois*.

GAN et al. (2015) concluded that muscle contraction across the centre of the sucker creates negative pressure, with the rim acting as a seal. However, they note that the friction areas most likely contribute to adhesion, with the relative importance of friction and suction being undetermined. Since these tadpoles move while still attached to the substrate, presumably the frictional forces must be overcome to achieve this.

Embryonic and larval staging: The only previous larval staging for an *Amolops* species that we have found, other than HORA's (1932) incomplete series, is PHAM et al.'s (2015) observations on eggs and larvae of *A. cremnobatus*. Hatching occurred at about stage 22, but larvae remained within the jelly mass adherent to rocks. HORA (1932) reported the prominent role of the cement gland during this phase, and that in a few individuals, the gland's regression was delayed until the sucker was more or less complete, implying some responsiveness to environmental conditions. *Amolops cremnobatus* larvae became active at stage 24, but remained within the jelly layer, now 9.5 mm long; during stage 25, larvae grew to 25 mm and were free of the jelly. By contrast, our *Amolops* sp. had progressed to stage 27/28 by 25 mm. PHAM et al.'s measurements on later stages are based on single specimens: they found that the tail began to shorten between stages 35 and 37 (we found continued growth up to stage 36, but had no later stages available), and that the lower tooth rows showed some atrophy by stage 42. By contrast, SCHLEICH & KÄSTLE (2012) reported tooth row degeneration at earlier stages in *A. marmoratus*, whereas NODZENSKI & INGER (1990) found that oral apparatus breakdown was delayed in comparison with generalist species in three gastromyzophorous species (previously *Amolops*, now *Meristogenys*), allowing these suctorial structures to remain functional during tail resorption. The maximum larval length for *A. cremnobatus* was a little more (47 mm at stage 35) than the maximum length we found by stage 36 (45 mm.); throughout larval growth, *A. cremnobatus* were longer than our specimens at comparable stages.

Species identity: The specimens described here originated from two different Nepalese rivers, a significant distance apart (Fig. 1). In our view, they represent the same species, because we could not find any significant morphological features to distinguish them. As well as providing combined data, we have given morphometric data from the two samples separately. Unfortunately, we have DNA evidence from only one of the locations. Five species of *Amolops* have been recorded from Nepal: *A. monticola*, *A. marmoratus*, *A. nepalicus*, *A. formosus* and the recently described *A. mahabharatensis*. In addition, NIDUP et al. (2016) have recorded *A. himalayanus* from Bhutan and it may have a wider distribution. SCHLEICH & KÄSTLE (2002) provide data on tadpoles of three of the species. The oral apparatus of *A. marmoratus* is said to be circular, with a smooth border, lacking papillae, and a LTRF of 8(4–8)/3(1) at earlier stages, altering to 6(3–6)/3(1) when hind limbs become well developed. *Amolops monticola* has an LTRF of 7(4–7)/3(1) and *A. nepalicus* 6(3–6)/3(1); no details are given of *A. formosus* tadpoles. From this comparison, our tadpoles are closest to

those of *A. marmoratus*, but with some clear differences: our specimens do have papillae on their lateral labia, and we have seen no decline in tooth row number up to stage 36, when limb buds are well developed. Our DNA analysis suggests that our specimens are closely related to *A. marmoratus* but not identical. Unfortunately, at the time of this study there were no Genbank sequences for *A. monticola*, *A. formosus*, or *A. himalayanus*. After the first revision of this study *A. nepalicus* was revalidated and *A. mahabharatensis* was described from a locality close to our study site (KHATIWADA et al., 2020). However, due to different genetic loci being used by ourselves and KHATIWADA et al. (12S vs 16S rDNA) and lack of genetic material for further sequencing being available, further comparison will have to wait until new sampling is undertaken and both gene fragments are sequenced from one individual to corroborate that our two samples are *A. mahabharatensis*. However, the very similar phylogenetic position and tadpole characteristics, such as the tooth row formula, as well as the geographic locality suggest that they likely are the same species.

Acknowledgements

We thank JEFF STREICHER for access to specimens in the NHM collections, MARGARET MULLIN for assistance with electron microscopy, MAGGIE REILLY (GLAHM) and TOBY HIBBITS (TCWC) for cataloguing material, SOFIA MOURÃO and PATRICIA RIBEIRO for laboratory assistance, and JON BARNES for kindly providing helpful comments on an earlier draft of the manuscript. KWC thanks RAJKAPUR NAPIT, KESHAV KHANAL and RICHARD MAYDEN for field assistance, and JIWAN SHRESTHA for help with fieldwork logistics and organizing permission from Department of National Parks and Wildlife Conservation to conduct scientific collecting in Nepal in 2008. This is publication #1625 of the Biodiversity Research and Teaching Collections of Texas A and M University. M.J.J. is supported by the Portuguese Foundation for Science and Technology (FCT, fellowship number SFRH/ BPD/109148/2015)

References

- AmphibiaWeb (2019): Online database accessible at <https://amphibiaweb.org>. – University of California, Berkeley, CA, USA. Accessed 31 January 2019.
- ALTIG, R. & G. F. JOHNSTON (1989): Guilds of anuran larvae: relationships among developmental modes, morphologies, and habitats. – *Herpetological Monographs*, **3**: 81–109.
- ALTIG, R. & R. W. McDIARMID (1999): Body plan: development and morphology. – pp. 24–51 in: McDIARMID, R. W. & R. ALTIG (eds): *Tadpoles – the biology of anuran larvae*. – University of Chicago Press, Chicago.
- CAI, H-X., J. C. CHEF, J-F. PANG, E. M. ZHAO & Y-P. ZHANG (2007): Paraphyly of Chinese *Amolops* (Anura, Ranidae) and phylogenetic positions of the rare Chinese frog, *Amolops tormotus*. – *Zootaxa*, **1531**: 49–55.
- CONWAY, K. W., D. E. EDDS, J. SHRESTHA & R. L. MAYDEN (2011): A new species of gravel-dwelling loach (Ostariophysi: Nemacheilidae) from the Nepalese Himalayan foothills. – *Journal of Fish Biology*, **79**: 1746–1759.
- DITSCHKE, P. & A. SUMMERS (2019): Learning from Northern clingfish (*Gobiesox maeandricus*): bioinspired suction cups attach to rough surfaces. – *Philosophical Transactions of the Royal Society, London B*, **374**: 20190204.
- DROTLEF, D. M., E. APPEL, H. PEISKER, K. DENING, A. DEL CAMPO, S. N. GORB & W. J. P. BARNES (2015): Morphological studies of the toe pads of the rock frog, *Staurois parvus* (family: Ranidae) and their relevance to the development of new biomimetically inspired reversible adhesives. – *Interface Focus*, **5**: 20140036.
- ENDLEIN, T., W. J. P. BARNES, D. S. SAMUEL, N. A. CRAWFORD, A. B. BIAW, & U. GRAFE (2013): Sticking under wet conditions: the remarkable attachment abilities of the torrent frog, *Staurois guttatus*. – *PLoS ONE*, **8**: e73810.
- FROST, D. R. (2020): Amphibian species of the world: an online reference: Version 6.0. – Electronic database accessible at <http://research.amnh.org/herpetology/amphibia/index.html>, accessed 6/7/2020. – American Museum of Natural History, New York, USA.
- GAN, L. L., S. T. HERTWIG, I. DAS & A. HAAS (2015): The anatomy and structural connectivity of the abdominal sucker in the tadpoles of *Huia cavitympanum*, with comparisons to *Meristogenys jerboa* (Lissamphibia: Anura: Ranidae). – *Journal of Zoological Systematics and Evolutionary Research*, **54**: 46–59.
- GOSNER, K. L. (1960): A simplified table for staging anuran embryos and larvae with notes on identification. – *Herpetologica*, **15**: 203–210.
- GOUY, M., S. GUINDON & O. GASCUEL (2010): SeaView version 4. A multiplatform graphical user interface for sequence alignment and phylogenetic tree building. – *Molecular Biology and Evolution*, **27**: 221–224.
- GREEN, D. M. & D. L. BARBER (1988): The ventral adhesive disc of the clingfish *Gobiesox maeandricus*: integumental structure and adhesive mechanisms. – *Canadian Journal of Zoology*, **66**: 1610–1619.
- HORA, S. L. (1930): Ecology, bionomics and evolution of the torrential fauna. – *Philosophical Transactions of the Royal Society, London B*, **218**: 172–281.
- HORA, S. L. (1932): Development and probable evolution of the suctorial disc in the tadpoles of *Rana afghana* Gunther. – *Transactions of the Royal Society of Edinburgh*, **57**: 469–472.
- HORA, S. L. (1934): Further observations on the bionomics of the tadpoles of *Rana afghana* Gunther. – *Records of the Indian Museum*, **36**: 321–325.
- JAVAHERY, S., H. NEKOUBIN & A. H. MORADLU (2012): Effect of anaesthesia with clove oil in fish. – *Fish Physiology and Biochemistry*, **38**: 1545–1552.
- KATO, K., K. MISAWA, K. KUMA & T. MIYATA (2002): MAFFT: a novel method for rapid multiple sequence alignment based on fast Fourier transform. – *Nucleic Acids Research*, **30**: 3059–3066.
- KHATIWADA, J. R., G. SHU, B. WANG, T. ZHAO, F. XIE & J. JIANG (2020): Description of a New Species of *Amolops* Cope, 1865 (Amphibia: Ranidae) from Nepal and Nomenclatural Validation of *Amolops nepalicus* Yang, 1991. – *Asian Herpetological Research*, **11**: 71–94.
- KOCHER, T. D., W. K. THOMAS, A. MEYER, S. V. EDWARDS, S. PAABO, F. X. VILLABLANCA & A. C. WILSON (1989): Dynamics of mitochondrial DNA evolution in animals: amplification

and sequencing with conserved primers. – Proceedings of the National Academy of Sciences of the U.S.A., **86**: 6196–6200.

MATSUI, M. & J. NABHITABHATA (2006): A new species of *Amolops* from Thailand (Amphibia, Anura, Ranidae). – Zoological Science, **23**: 727–732.

MILLER, M. A., W. PFEIFFER & T. SCHWARTZ (2010): Creating the CIPRES Science Gateway for inference of large phylogenetic trees. – pp. 1–8 in: Gateway Computing Environments Workshop (GCE).

MILLER, P. J. (1971): An elastin stain. – Journal of Medical Laboratory Technology, **28**: 148–149.

MITCHELL, M. A. (2009): Anesthetic considerations for amphibians. – Journal of Exotic Pet Medicine, **18**: 40–49.

NOBLE, G. K. (1929): The adaptive modifications of the arboreal tadpoles of *Hoplophryne* and the torrent tadpoles of *Staurois*. – Bulletin of the American Museum of Natural History, **58**: 291–334.

NIDUP, T., D. GYELTSHEN, PENJOR, S. DORJI & M. J. PEARCH (2016): The first record of *Amolops himalayanus* (Anura: Ranidae) from Bhutan. – Herpetological Bulletin, **136**: 13–18.

NGO, A., R. W. MURPHY, W. LIU, A. LATHROP & N. I. ORLOV (2006): The phylogenetic relationships of the Chinese and Vietnamese waterfall frogs of the genus *Amolops*. – Amphibia-Reptilia, **27**: 81–92.

NODZENSKI, E. & R. F. INGER (1990): Uncoupling of related structural changes in metamorphosing torrent-dwelling tadpoles. – Copeia, **1990**: 1047–1054.

OHLER, A. (1995): Digital pad morphology in torrent-living Ranid frogs. – Asiatic Herpetological Research, **6**: 85–96.

PHAM, C. T., A. DOGRA, A. GAWOR, A. RAUHAUS, G. KLOEBLE, T. Q. NGUYEN & T. ZIEGLER (2015): First record of *Amolops cremnobatus* from Thanh Hoa province, Vietnam, including an extended tadpole description and the first larval staging for *Amolops*. – Salamandra, **51**: 111–120.

POSADA, D. (2008): jModelTest: phylogenetic model averaging. – Molecular Biology and Evolution, **25**: 1253–1256.

RONQUIST, F. & J. P. HUELSENBECK (2003): MrBayes 3: Bayesian phylogenetic inference under mixed models. – Bioinformatics, **19**: 1572–1574.

SAMBROOK, J., E. F. FRITSCH & T. MANIATIS (1989): Molecular Cloning: A Laboratory Manual, second ed. – Cold Spring Harbor Laboratory Press, New York.

SCHLEICH, H. H. & W. KÄSTLE (eds) (2002): Amphibians and Reptiles of Nepal. – ARG Gantner Verlag Kommanditgesellschaft, Liechtenstein.

SILVESTRO, D. & I. MICHALAK (2012): RaxmlGUI: a graphical front-end for RAXML. – Organisms, Diversity and Evolution, **12**: 335–337.

SUBHA, B., N. A. ARAVIND & G. RAVIKANTH (2016): Amphibians of the Sikkim Himalaya, India: an annotated checklist. – CheckList, **13**: 2033.

WAINWRIGHT, D. K., T. KLEINTEICH, A. KLEINTEICH, S. N. GORB & A. P. SUMMERS (2013): Stick tight: suction adhesion on irregular surfaces in the northern clingfish. – Biology Letters, **9**: 20130234.

YANG, D. T. (1991): Phylogenetic systematics of the *Amolops* groups of ranid frogs of southeastern Asia and the Greater Sunda Islands. – Fieldiana Zoology (NS), **1423**: 1–42.

Supplementary data

The following data are available online:

Supplementary document S1. Dimensions of *Amolops* sp. tadpoles sample, arranged by GOSNER (1960) stage for the two samples separately.